AN INDOOR LOCALIZATION METHOD FOR MOBILE ROBOT USING CEILING MOUNTED APRILTAGS

Van Tien Hoang[1], Quoc Nam Tang[1], Xuan Tung Truong[2], Dinh Quan Nguyen[1,*]

[1]*Faculty of Aerospace Engineering, Le Quy Don Technical University, Hanoi, Vietnam;*

[2]*Faculty of Control Engineering, Le Quy Don Technical University, Hanoi, Vietnam*

Abstract

Localization is one of the most important functions for autonomous mobile robots (AMRs). For indoor applications, the localization problem faces some difficulties such as lightning variation, dynamic objects or highly reflective surfaces that generate measurement noises for the perceptive sensor systems. Recently, tags-based pose estimation has become a popular and efficient solution for AMRs. In this article, we also ultilize ceiling mounted AprilTags for our AMR application in indoor environment. The advantage of AprilTags is their invariance to uncertainty of the environment such as lightning conditions, providing robust pose measurements with a fairly large range of measuring distances from the camera to fiducial markers. By integrating AprilTags in the SLAM package, we have solved several problems such as robot pose-recovery problem and improving the accuracy of the robot localization. Experiments with an AMR robotic system, the Vibot-2 robot, are carried out in two cases: under day-light condition and night-time condition to verify the accuracy of the method. In addition, we also discuss our solution of tag positioning in order to increase the stability of the robot navigation in global map. Experiment results show that the accuracy in pose estimation is less than 20 cm in terms of position and less than 5° in terms of heading angle. Furthermore, the pose measurements from the camera are quite stable under different lightning conditions.

Keywords*: Autonomous mobile robot; localization; navigation; AprilTags.*

1. Introduction

In the past decades, localization has been a hot research topic in the field of autonomous mobile robots. A mobile robot without a good pose estimator can not work properly in a dynamic working environment. It is a complicated problem that requires many information from various sensor sources and advanced fusion algorithms to solve.

Conventional localization methods for outdoor applications often used the extended Kalman filter to estimate the position and orientation of the robot based on feedback data coming from wheel encoders, IMU or GPS which can provide reliable measurements [1]. However, for indoor applications, the task of positioning the robot in the global map becomes much more complicated under dynamic working environment.

[*] Email: ndquan@lqdtu.edu.vn
https://doi.org/10.56651/lqdtu.jst.v17.n05.531

The AMRs need to use not only encoders, IMU but also other advanced sensor devices such as 2D or 3D laser range finders (LiDAR), 2D or 3D cameras, indoor GPS,…

Up to now, some of the most practical approaches to solve the localization of AMRs are from probablistic robotics [2]. These approaches use particle filter-based positioning (PF) to represent a state in which a robot can appear in the global map, then uses a particle filter to calculate and converge the particles to a point about the actual position of the robot. Among them, AMCL is currently the most effective and popular algorithms that use particle filters [3, 4]. Due to large computation load, this algorithm has a slow position convergent speed, especially when the robot's initial position is unknown [5]. The work in [6] introduced a vector based AMCL for indoor maps which ultilizes line segments from vector-based CAD floor plans to process for pose estimation instead of using conventional grid maps, which could increase the efficiency in terms of memory usage and accuracy. Lately, a positioning method based on learning algorithms is used in conjunction with AMCL to accelerate global positioning in a wide operating environment [7].

Despise the fact that AMCL is very powerful, there are cases it fails to provide a stable estimation for the robot position. If, for example, due to some mismatches, the robot lost its position on the map (kidnapping problem), it will be very difficult to recover the robot position in a short time based only on the information from odometry and lidar sensors. In order to overcome this drawback, many studies have integrated additional features to fuse with AMCL (which based mainly on lidar sensors) [8-19].

WiFi signal transmitters are used to estimate the initial position of the robot for the AMCL algorithm to reduce the calculation time and increase the global positioning accuracy of the indoor robot [8, 9]. Fiducial markers are used in combination with data from lidar to add more environmental features can increase the efficiency of positioning in the global map and solve the problem of abduction of indoor robots [10]. The work in [11] used RGBD camera and AprilTags at wall-mounted landmarks in combination with AMCL algorithm to speed up global positioning and reduce uncertainty in location tracking, and solve robot kidnapping problem. The concept of using moving tags that are mounted on moving objects in the environment is also carried out, for example in [16].

Several techniques of pose estimation based on fiducial markers are compared in [12]. Among them AprilTags are one of the most commonly used fiducial markers that can be used both indoor and outdoor for ground truth generation in 6-DOF pose estimation. The AprilTags were first introduced in 2011 in [14] and later have been improved with new tag library, AprilTag 2 in [15] and AprilTag 3 in [16].

In most of the applications that integrate AprilTags, the robot localization is mainly based on the 6-DOF pose estimation of the tags (or tag bundle) with respect to the camera frame via the Perspective-n-Point (PnP) algorithm [16-18]. This method has several advantages: (1) it allows us to determine full coordinates in the tag space; (2) can be applied in the case of large distance and field of view (as long as the tag can be read). However, it requires large computation and the accuracy depends greatly on the distance and viewing angle from the camera with respect to the tags. Besides, in most of the studies, for example in [13, 18, 19], the AprilTags are attached along the side wall or on the floor along side the robot path quite densely. In theory, the more tags are there, the more information the robot can get thus provides more accuracy for the robot localization. But this way of positioning the fiducial tags in the surrounding is not always practical because it affects the aesthetics of the environment and in some cases it is not really efficient.

In this article, we use a completely different approach to compute the robot pose based on AprilTags in the global map. The experiments have been carrried out with the Vibot-2 AMRs in indoor environments which are the quarantine areas for Covid-19 patients in some hospitals in the North and South of Vietnam (during the pandemic periods in 2020 and 2021). In our solution, we have attached the AprilTags to the ceiling of the lobbies in the buildings where the robots perform some delivery tasks automatically (i.e. providing foods, medicines and neccessary for the patients). Instead of using 6-DOF pose of the tags, we determine the robot position based on the calculation of the 3-DOF pose of the robot camera in the tag frame via some transformations between planar coordinates frames. This method gives us a fast, reliable solution and has better accuracy compared to the 6-DOF pose estimation using PnP solver.

In the second part, we describe our localization problem and the 3-DOF pose calculation using ceiling mounted AprilTags. Solution for the kidnapping problem is presented in Section 3. Our proposed method for improving the global localization is discussed in detail in Section 4. Section 5 shows some experiments to verify the accuracy and stability of our pose estimation based on AprilTags under different lightning conditions.

2. Indoor localization using ceiling mounted AprilTags

2.1. The Vibot-2 AMR system

The Vibot-2 AMR is an intelligent medical transportation robot capable of self-mapping, navigating, avoiding dynamic and static obstacles, automatically receiving and returning goods and returning to the charging station when the battery runs out. Robots are used in quarantine areas with a high risk of infection to replace medical staff

in transporting food, medicine, necessities, collecting garbage and supporting remote medical examination through video calls. Each robot Vibot-2 has been equipped with suitable actuators and sensor system.

Figure 1 shows the hardware components of the robot and one prototype working in a hospital. The mobile base is designed with type (2,0) structure including: two active fixed wheels are placed at the middle of the base frame and having the wheel radius of 0.075 m, four castor wheels are placed at the four coners of the base frame to support the robot body. Each active wheel is driven by a 120W BLDC servo motor with a maximum speed of 3000 rpm and connecting to a gear box with 1:30 gear ratio to increase the output moment. This combination allows the robot to move with a maximum speed of 0.8 m/s and carry large payloads up to 120 kg. One lifting table is attached to the base frame to get the carts at the cart stations. The lifting mechanism is our new design solution which uses a linear actuated cylinder to lift up and down all the delivery carts.

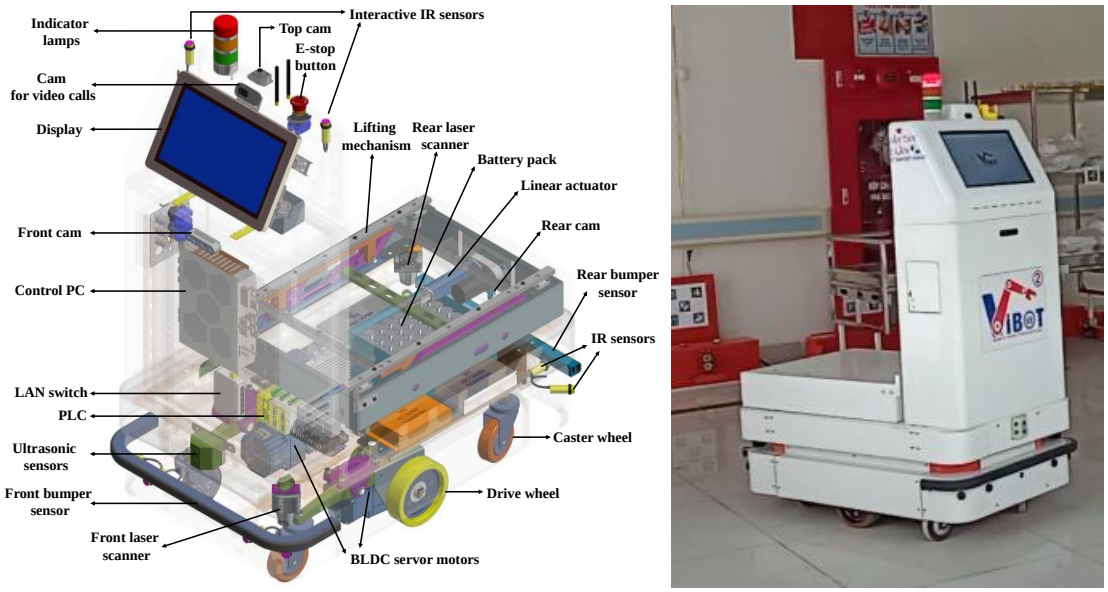

Fig. 1. Vibot-2 AMR system:
(a) The hardware of Vibot-2 AMR; (b) A Vibot-2 AMR is working at Bac Giang general.

Each Vibot-2 AMR has a navigation system consisting of various sensors: encoders on wheel-drive motors, a UM7 inertial measuring unit (data from encoders and IMU are processed with an extended Kalman filter to get odometry information); two SICK TIM551 lidars (placed diagonally front and rear to allow a full 360° scanning

range of the robot's environment). Ultrasonic sensors, several IR sensors and two bumper sensors are placed around the robot base to increase the safety of the robot. There are four cameras in the robotic system including:

- One camera (720p, 30fps, 65° FOV) is mounted on top of the control cabin facing the ceiling to read the AprilTag codes.
- One front camera is used to look for the delivery cart. We also use AprilTag on the carts so that the robot can recognize the correct cart for a given delivery task (see Fig. 1b).
- One rear camera is used to aid the robot in docking phases (i.e. returning to the charge station or moving into the cart stations).
- One camera is used for remote video calls for telecommunication between doctors and patients via the robot.

The robot localization and navigation packages are running on an industrial PC with an Intel Quad Core i7 8550U (1.80GHz) CPU and 16GB of RAM.

2.2. Global localization using AprilTags

The localization of Vibot-2 AMR consists of three stages:

- Computing the robot odometry which is a fusion from a kinematic based estimator using wheel encoder feedback together with an IMU to get heading angle.
- Computing the robot pose via AMCL package with the inputs coming from the robot odometry and point cloud of distances provided by lidar devices as well as a global map of the floor plan.
- Re-correct the robot pose in global map using fixed fiducial markers that are attached to the ceiling of the robot working environment.

In this section, we only focus on the use of AprilTags to compute the 3-DOF pose of the robot in global map. With the high computing performance of the Vibot-2 computer, the AprilTag 3 library are selected to ensure the highest efficiency in terms of detection speed and positioning accuracy with small sized tags [16].

To position the Vibot-2 AMR in the global map, the AprilTag of type 36h11 with size 10.5 × 10.5 [cm] is used to assign fixed global coordinates and is affixed to

the ceiling so that the tag's conventional axes, as seen in Fig. 2, coincides with the global coordinate system associated with the map, as depicted in Fig. 3.

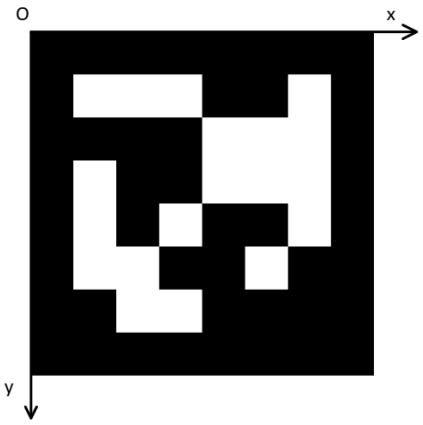

Fig. 2. An AprilTag with ID 03 with assigned local coordinate frame Oxy, the origin point O has global coordinates (x = 4.21 m, y = -3 m, θ = 0 deg).

Fig. 3. AprilTags are mounted on the ceiling at Bac Giang general hospital.

When the AprilTag is read on the ceiling, the robot stops, determines the coordinates and direction of the robot in the global map from the global coordinates and directions assigned to the tag, as seen in Fig. 4.

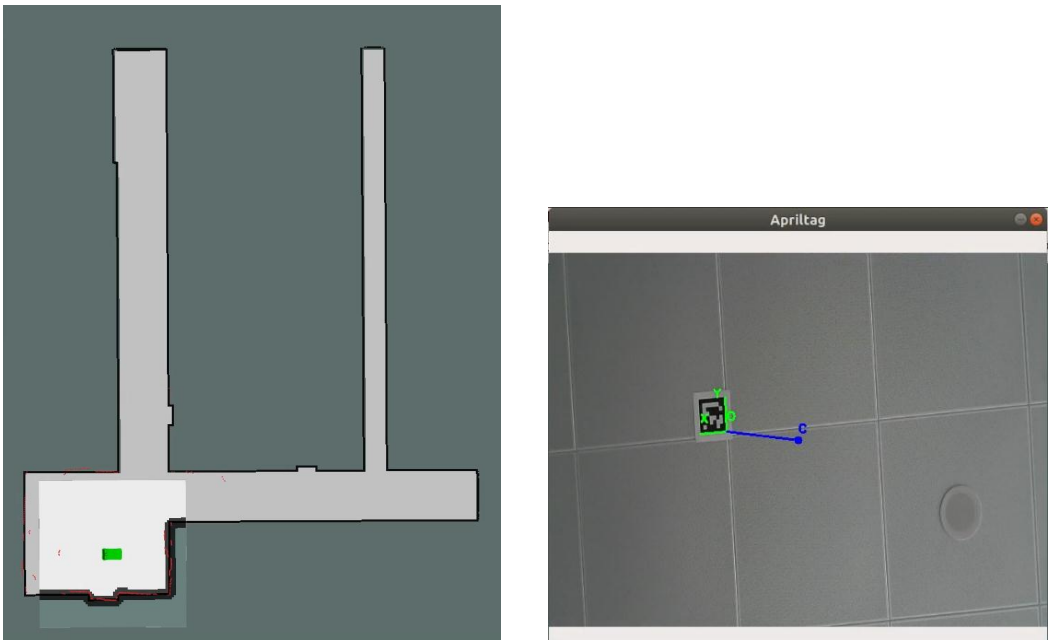

(a) Global map *(b) AprilTag reading window*

Fig. 4. Robot read the AprilTag with ID 03 and re-locating its position on the global map.

In Fig. 4, when the tag is read, the coordinates of 3 points O, X, Y (3 corners of the tag) and point C (the center of the camera frame is also the center of the camera) in the image coordinate system will be determined.

In Fig. 5, the $O_IX_IY_I$ coordinate system is the image coordinate system; position of the AprilTag corresponding to $O_1X_1Y_1$ when the robot's orientation angle in the global coordinate system is zero; position $O_2X_2Y_2$ corresponding to the direction angle theta; *deltaX* and *deltaY* are the differences of the coordinates of the point X and the point O on the O_IX_I and O_IY_I axes, respectively.

Since the OX edge of the tag is glued to the ceiling so that it is parallel to the x-axis of the global coordinate system attached to the map, when the robot heading angle in the global coordinate system is zero, the angle of the OX in the image coordinate system is equal to -90° corresponding to the position O_1X_1 as shown in Fig. 5. Therefore, the robot's orientation angle in the global map can be calculated by the rotation of the OX edge from the O_1X_1 in the image coordinate system but in the opposite direction.

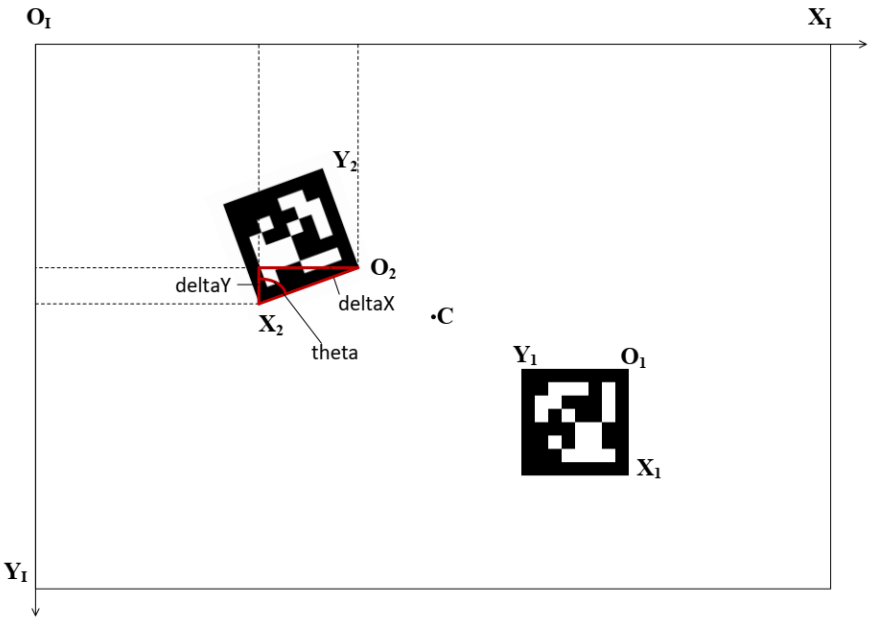

Fig. 5. Determine the robot heading angle in global coordinate frame.

The heading angle of the robot is determined as follows:

$$\theta = -\left[\arctan\left(deltaY / deltaX\right) - \frac{\pi}{2}\right] \quad (1)$$

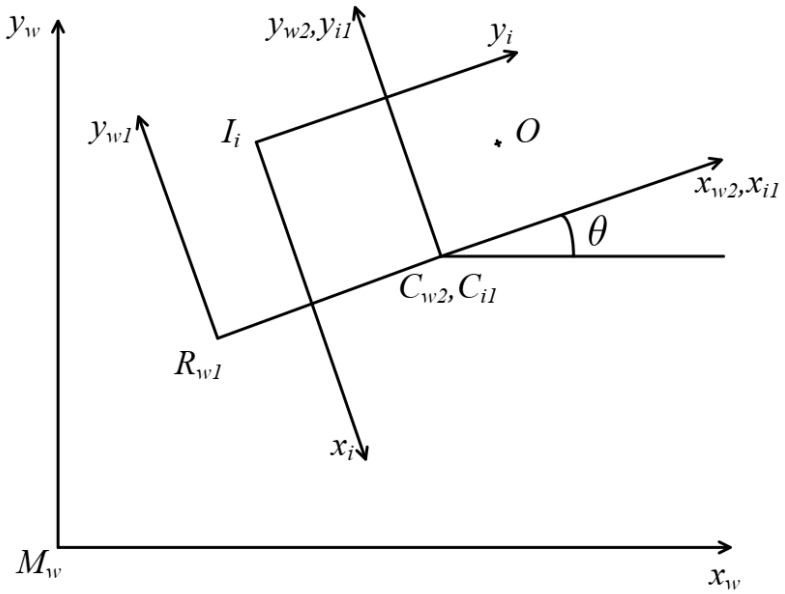

Fig. 6. Determine the robot position in global coordinate frame.

To get the robot position in the global coordinate frame, firsly, we determine the camera center point (point C) in the global frame via coordinate transformations from image coordinate system $I_i x_i y_i$ to the real coordinate system $E_w x_w y_w$. From then it is posible to calculate the robot pose in the global frame.

Figure 6 describes the coordinate frames:

- The global coordinate frame attached to the map $M_w x_w y_w$;
- The coordinate frame attached to the robot $R_{w1} x_{w1} y_{w1}$;
- The coordinate frame attached to the camera center point $C_{w2} x_{w2} y_{w2}$. The axes $C_{w2} x_{w2}$ and $R_{w1} x_{w1}$ are coincided, the axis $C_{w2} y_{w2}$ is parallel to $R_{w1} y_{w1}$;
- The coordinate frame $C_{i1} x_{i1} y_{i1}$ is attached to the camera at point C but is expressed in the image space (unit pixels) having all axes coincide with $C_{w2} x_{w2} y_{w2}$;
- The image coordinate system $I_i x_i y_i$ has a size of 640×480 pixels. The camera center point C is placed at the center of the image frame, as seen in Fig. 6;
- The coordinates of the point O on the AprilTag are given in the global coordinate frame and in the image coordinate frame: $\left(x_O^{(w)}, y_O^{(w)}\right), \left(x_O^{(i)}, y_O^{(i)}\right)$.

We have:

$$\begin{bmatrix} x_O^{(i1)} \\ y_O^{(i1)} \end{bmatrix} = \begin{bmatrix} x_I^{(i1)} \\ y_I^{(i1)} \end{bmatrix} + \begin{bmatrix} \cos\left(-\frac{\pi}{2}\right) & -\sin\left(-\frac{\pi}{2}\right) \\ \sin\left(-\frac{\pi}{2}\right) & \cos\left(-\frac{\pi}{2}\right) \end{bmatrix} \begin{bmatrix} x_o^{(i)} \\ y_o^{(i)} \end{bmatrix} \tag{2}$$

or

$$\begin{cases} x_O^{(i1)} = -240 + y_O^{(i)} \\ y_O^{(i1)} = 320 - x_O^{(i)} \end{cases} \tag{3}$$

Projecting the coordinates of point O from image frame to the real coordinate frame we have:

$$\begin{bmatrix} x_O^{(w2)} \\ y_O^{(w2)} \end{bmatrix} = k \begin{bmatrix} x_O^{(i1)} \\ y_O^{(i1)} \end{bmatrix} \tag{4}$$

where *k* is the conversion ratio between the image unit pixel to the real coordinate unit:

$$k = \frac{|OX|_r}{|OX|_i} \tag{5}$$

with $|OX|_r = 0.105\,[\mathrm{m}]$ is the real dimension of the OX edge of the AprilTag and $|OX|_i$ is the dimension in pixel of the OX edge in the image frame.

Projecting the point O from the frame $C_{w2}x_{w2}y_{w2}$ to $M_w x_w y_w$ we have:

$$\begin{bmatrix} x_O^{(w)} \\ y_O^{(w)} \end{bmatrix} = \begin{bmatrix} x_C^{(w)} \\ y_C^{(w)} \end{bmatrix} + \begin{bmatrix} \cos(\theta) & -\sin(\theta) \\ \sin(\theta) & \cos(\theta) \end{bmatrix} \begin{bmatrix} x_O^{(w2)} \\ y_O^{(w2)} \end{bmatrix} \tag{6}$$

And we get the camera center point in the global coordinate frame:

$$\begin{bmatrix} x_C^{(w)} \\ y_C^{(w)} \end{bmatrix} = \begin{bmatrix} x_O^{(w)} \\ y_O^{(w)} \end{bmatrix} - \begin{bmatrix} \cos(\theta) & -\sin(\theta) \\ \sin(\theta) & \cos(\theta) \end{bmatrix} \begin{bmatrix} x_O^{(w2)} \\ y_O^{(w2)} \end{bmatrix} \tag{7}$$

where $\left(x_O^{(w)}, y_O^{(w)}\right)$ are the coordinates of the point O of the fixed AprilTag which are given in the global frame, the heading angle θ is computed from (1) and $\left(x_O^{(w2)}, y_O^{(w2)}\right)$ are determined from (4).

The robot coordinates are computed from the camera center point as follows:

$$\begin{bmatrix} x_R^{(w)} \\ y_R^{(w)} \end{bmatrix} = \begin{bmatrix} x_C^{(w)} \\ y_C^{(w)} \end{bmatrix} - \begin{bmatrix} \cos(\theta) & -\sin(\theta) \\ \sin(\theta) & \cos(\theta) \end{bmatrix} \begin{bmatrix} x_C^{(w1)} \\ y_C^{(w1)} \end{bmatrix} \tag{8}$$

With $x_C^{(w1)} = |RC| = 0.263\ m$ and $y_C^{(w1)} = 0$ we have:

$$\begin{cases} x_R^{(w)} = x_C^{(w)} - 0.263 \cdot \cos(\theta) \\ y_R^{(w)} = y_C^{(w)} - 0.263 \cdot \sin(\theta) \end{cases} \tag{9}$$

3. Robot pose recovery

During our demo tests at the research center, we have tried out several techniques with AMCL as the core for the robot pose estimator and have experienced many lost position situations. Figure 7 shows a floor plan of our testing environment for the Vibot-2 AMR. The longest distance is about 60 m which is quite a large area. The building floor has a symetric structure which means there are similar areas in the two sides of the map. This feature indeed created problems for our AMCL algorithm. When there is no fixed fiducial marker, the algorithm tends to fail to provide accurate coordinates in the global map after one or two hours of continuously running around, especially when the robot move to areas with a lot of similarity construction features. In such cases, the robot position could be switched in either sides of the global map and it

also lost the heading as well. This condition led to weird moving behaviors or the robot would just stop moving while looking for a new valid path.

The main reasons for the kidnapping state of the robot can be: (1) the cumulative errors of the odometry calculator, (2) the mismatch in AMCL while matching similar sections in global map and (3) the measurement noise from environment conditions such as drifting floor, poor lightning, reflective surfaces… It is important to take the robot out of kidnapping state or prevent it for not falling in this state to ensure proper operations. Using fixed fiducial markers as reference to recover the robot pose is one of the most practical solutions for this problem.

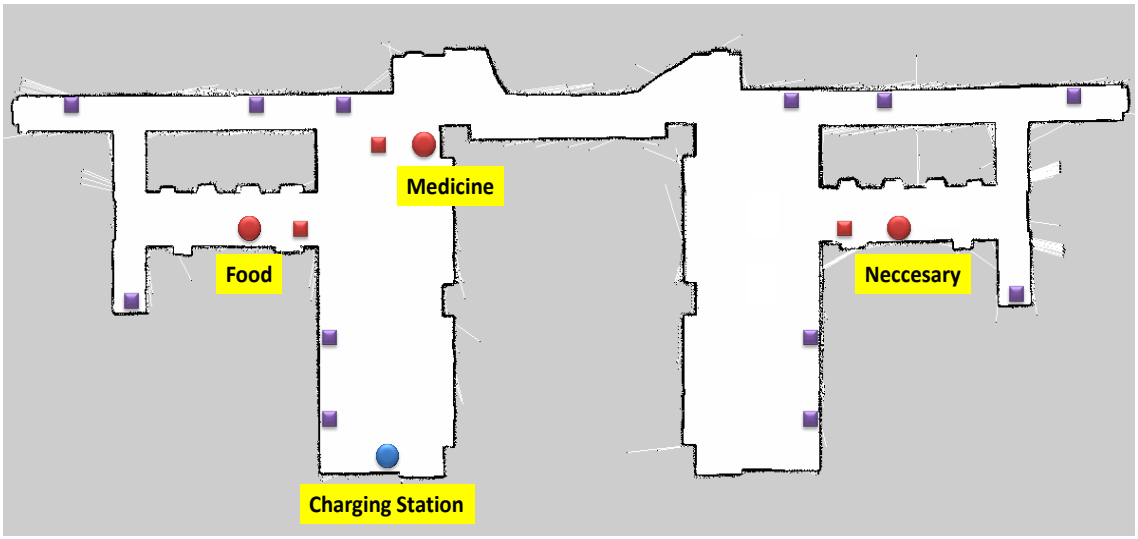

Fig. 7. A tag positioning solution for Vibot-2 AMR - 2nd floor of S1 building in Le Quy Don Technical University.

Figure 8 shows our algorithm to recover a robot pose when it falls into a lost position state. During operation, if the output of robot global localization algorithm is misplaced, the robot will be misguided, it cannot find the way to the desired destination, move slowly around a position or stop. This feature is used to detect and notify the robot of losing its position on the map. In case where the robot is kidnapped by the user (e.g. move the robot to a new location), the user will notify the robot of the abduction status via the console. When the robot realizes the status is lost or kidnapped, the automatic pose recovery mode using AprilTag will be activated to help the robot re-locate the position on the map and continue to perform the previous autonomous mission or wait for a new task.

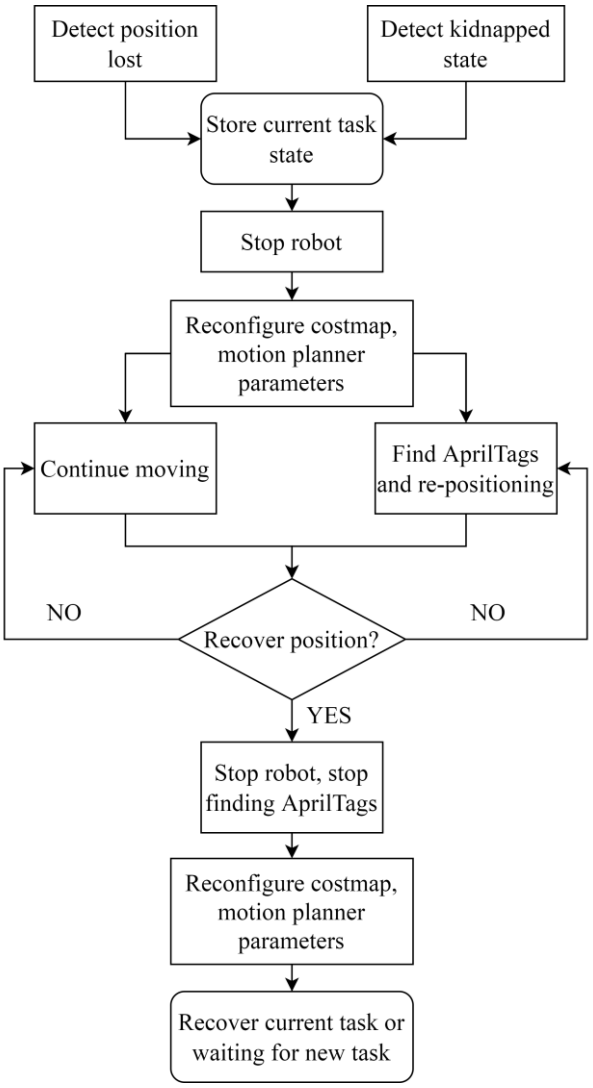

Fig. 8. Re-locating algorithm after a position lost or kidnapping state of the Vibot-2 AMR.

4. Improve the global localization using AprilTags

For Vibot-2 AMR, we ultilize the advanced AMCL as the core technique for global localization of the robot on a predefined static working map. This technique takes into account all the information from basic odometry, lidar sensors and static map to calculate the robot current pose. For environment with rich landmark features, this algorithm usually provides good estimations. However, for maps with repetitive structures this method sometimes fails to give correct information of the robot pose which leads to lost of position state and hard to recover from as mentioned in the previous section.

In order to improve the stability of the AMCL algorithm, we develop a fusion scheme where information getting from the AprilTags is used to increase the accuracy and stability in estimating the robot pose. Figure 9 shows the fusion scheme. Whenever the robot performed a sucessfully reading from an AprilTag, the new pose information is then fed into the AMCL algorithm via the node "initial_pose". This node is acting like a reference for the AMCL to update its starting guess of the robot location on the global map within each computation loop.

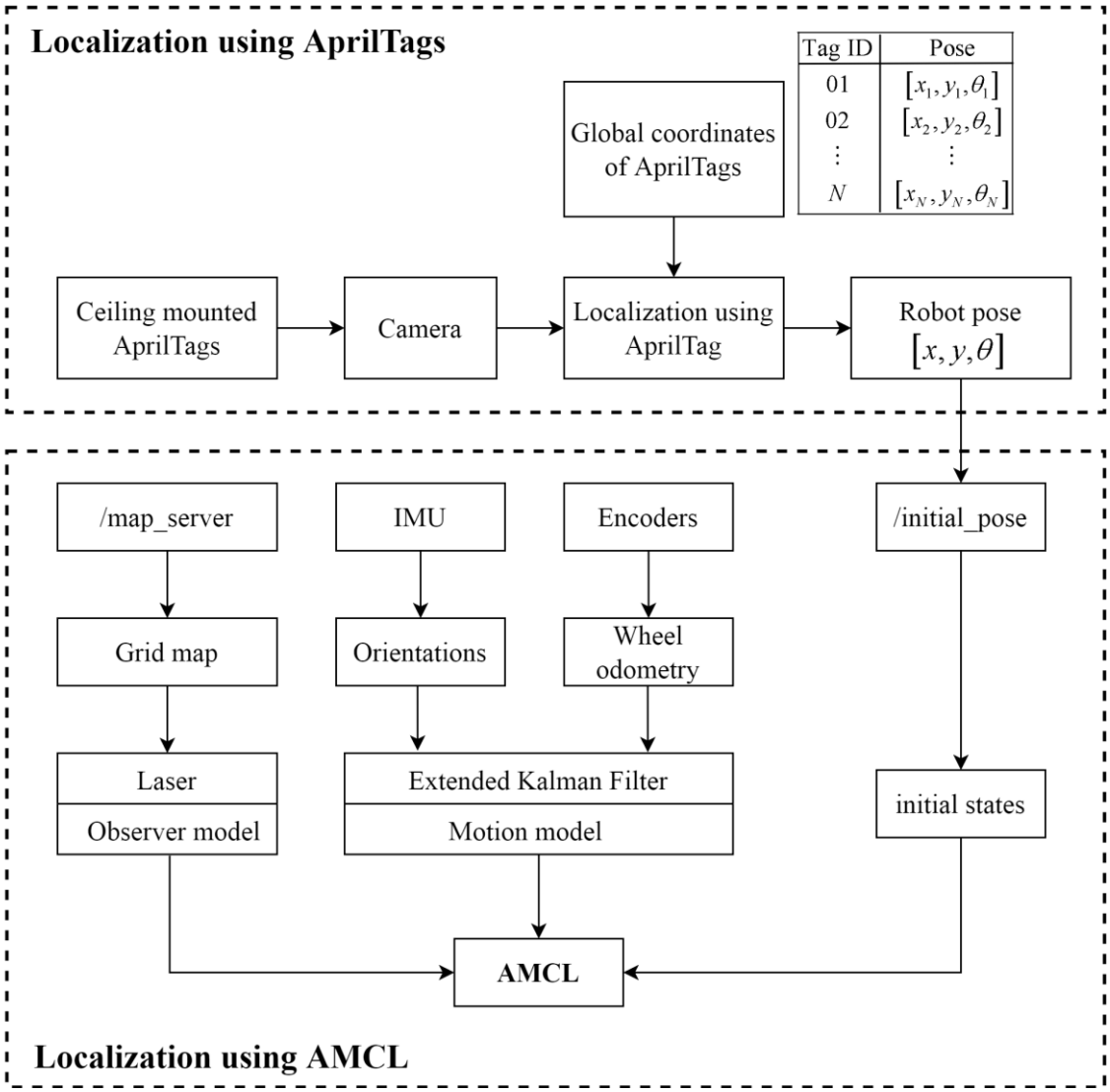

Fig. 9. Integrating AprilTag in robot global localization.

Note that the AprilTag reading only provides reference for global localization at specific places where the tags are mounted. Between any two consecutive readings the robot still need to calculate its pose based on information getting from laser sensors and basic odometry. The tag reading is necessary to reduce the errors due to localization model and sensor biases (or sensor drifting) over time.

There is a question need to be answered: *How can the tags be positioned to get a good outcome*? When the robot lost its position, if there are a lot of tags attached to the ceiling, it is easier for the robot to recover its pose on the map. However, a lot of tags will not be a favorite solution since this will affect the aesthetic of the building structure and not all of the admistrators will allow us to freely attach random tags to the ceiling of the working areas. For this problem, we only placed the AprilTags at specific locations where the robot must stop to perform some tasks during its operation, for example in front of each room in the building, in front of the cart stations or at charging station (see Fig. 7). The normal distance between two consecutive tags are around $10 \div 20$ m. And the tags are placed on the main routes of the robot when it performs its daily delivery tasks.

At the places where there could be many changes to the environment conditions such as water are frequently spilled onto the floor, we need to increase the density of the tags in order to increase the valid reading probability of the robot if in case a slippage might lead to a miscalculation of the pose estimator. Figure 3 shows an example of this case at Bac Giang hospital (we placed four AprilTags at the area of supplying carts, but use only two AprilTags along the two lobbies of the quarantine area in Fig. 4a).

5. Experiment

In this section, we will show some experiment results with the Vibot-2 AMR. The position of the robot is updated via the AprilTag reading. The vertical distance from the camera to the AprilTags is 1.5 m. The size of the AprilTag mounted on the ceiling is a square of 0.105×0.105 [m]. The camera field of view is 65° and we used non-distorted camera lense.

Figure 10 and 11 show the experiment setup for the tag reading under day-light and night-time conditions. At each testing position of the robot, we get the robot poses measured from the 3-DOF pose tag-based reading algorithm. The results are compared with the exact pose in global map. Two laser levels are used for re-positioning the AprilTags at correct position and orientation with respect to the global coordinate frame (see Fig. 12).

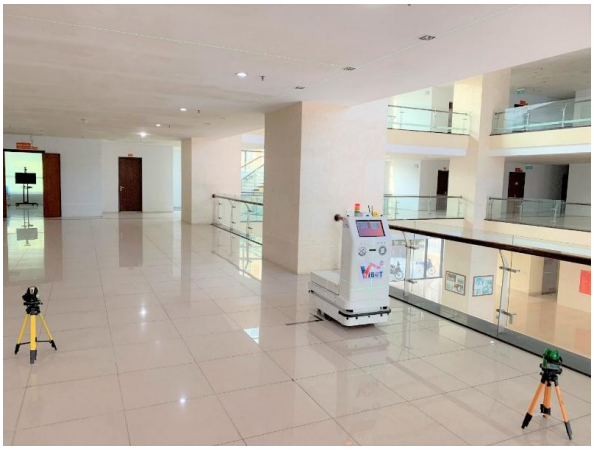

Fig. 10. Setting up the experiment under day-light condition.

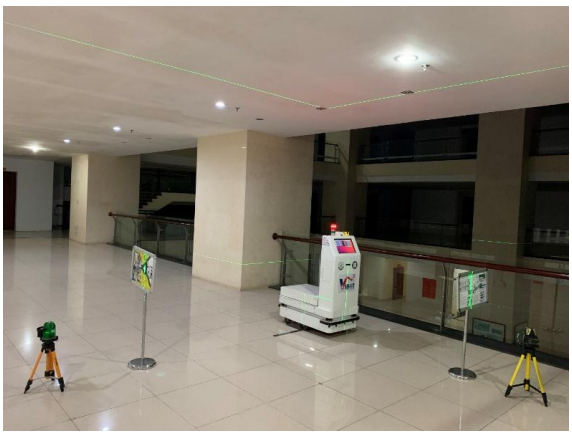

Fig. 11. Setting up the experiment under night-time condition.

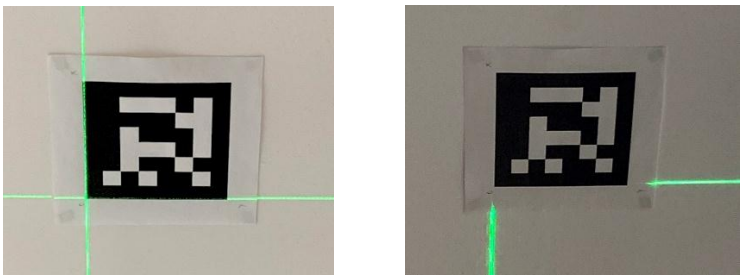

(a) *(b)*

Fig. 12. AprilTag with ID = 20 is attached at coordinates x = 4.66 m, y = -2.7 m, θ = 0 deg: (a) under day-light condition, (b) under night-time condition.

Figure 13 and 14 show the image frame captured during the experiments in the two different lightning conditions at the coordinates x = 4.66 m, y = -2.7 m with four different heading angles.

P1: θ = 0 *deg* P2: θ = 90 *deg*

P3: θ = 180 *deg* P4: θ = 270 *deg*

Fig. 13. AprilTag with ID = 20 is attached at coordinates x = 4.66 m, y = -2.7 m, under day-light condition.

P1: θ = 0 *deg* P2: θ = 90 *deg*

P3: θ = 180 *deg* P4: θ = 270 *deg*

Fig. 14. AprilTag with ID = 20 is attached at coordinates x = 4.66 m, y = -2.7 m, under night-time condition.

Figure 15 and 16 show the image frame captured during the experiments in the two different lightning conditions, having small distances between the tag center and camera center (image center).

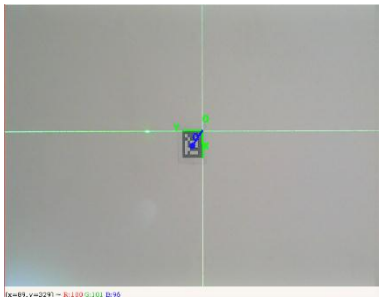

P5: x = 4.5 m, y = -2.7 m, θ = 0 deg

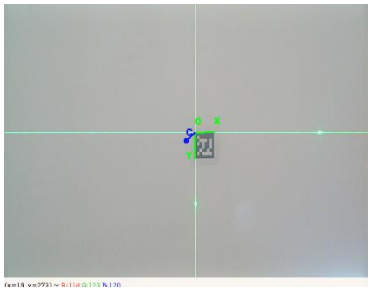

P6: x = 4.66 m, y = -2.898 m, θ = 90 deg

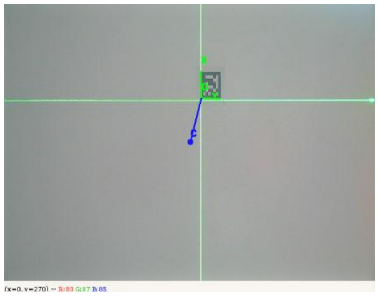

P7: x = 4.765 m, y = -2.7 m, θ = 180 deg

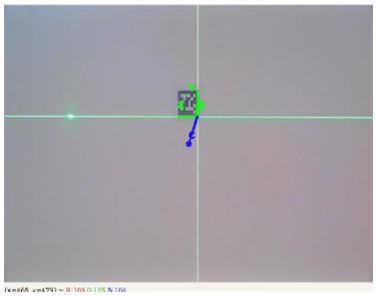

P8: x = 4.66 m, y = -2.515 m, θ = 270 deg

Fig. 15. Experiments under day-light condition with small distances between tag center and camera center.

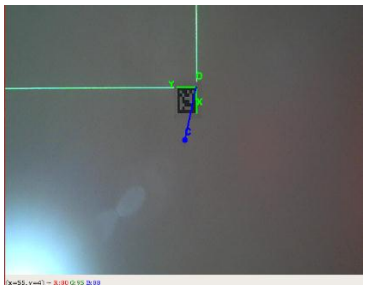

P5': x = 4.565 m, y = -2.7 m, θ = 0 deg

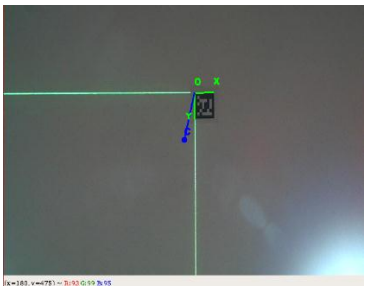

P6': x = 4.66 m, y = -2.77 m, θ = 90 deg

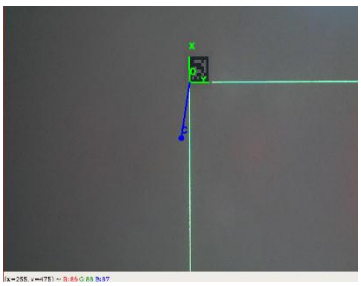

P7': x = 4.73 m, y = -2.7 m, θ = 180 deg

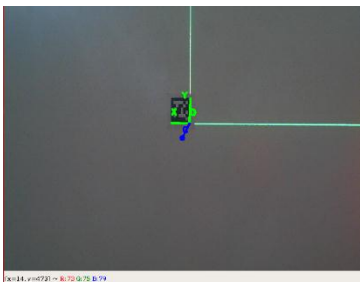

P8': x = 4.66 m, y = -2.55 m, θ = 270 deg

Fig. 16. Experiments under night-time condition with small distances between tag center and camera center.

Table 1 shows the errors between measured poses and the exact poses in the experiments under day-light and night-time conditions. The errors are computed with $\Delta\theta = \theta_{mea} - \theta_{ref}$ and $\Delta d = \sqrt{\left(x_{mea} - x_{ref}\right)^2 + \left(y_{mea} - y_{ref}\right)^2}$.

Table 1. List of real pose measurements using AprilTags of the Vibot-2 AMR

Cases	**Poses**	**Errors**	**Day-light**	**Night-time**
1	P1	$\Delta\theta$ (*deg*)	1.1	1.2
		Δd (*m*)	0.077	0.05
2	P2	$\Delta\theta$ (*deg*)	1.5	1.4
		Δd (*m*)	0.158	0.139
3	P3	$\Delta\theta$ (*deg*)	1.2	1.2
		Δd (*m*)	0.071	0.066
4	P4	$\Delta\theta$ (*deg*)	1.2	1.1
		Δd (*m*)	0.147	0.147
5	P5	$\Delta\theta$ (*deg*)	1.2	
		Δd (*m*)	0.066	
6	P6	$\Delta\theta$ (*deg*)	1.7	
		Δd (*m*)	0.037	
7	P7	$\Delta\theta$ (*deg*)	1.3	
		Δd (*m*)	0.058	
8	P8	$\Delta\theta$ (*deg*)	1.4	
		Δd (*m*)	0.046	
9	P5’	$\Delta\theta$ (*deg*)		1.2
		Δd (*m*)		0.072
10	P6’	$\Delta\theta$ (*deg*)		1.7
		Δd (*m*)		0.07
11	P7’	$\Delta\theta$ (*deg*)		1.3
		Δd (*m*)		0.055
12	P8’	$\Delta\theta$ (*deg*)		1.4
		Δd (*m*)		0.039

The results in the Tab. 1 show that the pose errors (position errors and heading angle errors) under day-light condition are not much different from under night-time

condition. The pose reading based on AprilTags is not being affected greatly under various lightning conditions.

Table 2 shows the results of errors between measurement values and real robot poses in experiments with different distances between the tag center and image center. It can be seen that, in the case the tag center is far from the image center we get large errors in absolute coordinates (x, y). This is because at the image area far from the image center, the image of tag is tent to be distorted more (radial distortion). However, this changes do not affect much on the reading of robot heading angle. Besides, at the poses where the heading angle θ is closed to 90° and 270° the position errors are quite big (nearly doubled compared to other poses). In equation (5), the coefficient k is calculated with respect to the OX axis of the tag but in reality, the conversion ratios with respect to the OX and OY axes of the tag are different (it can be seen on Fig. 13 ÷ 16). Specifically, at the poses with θ closed to closed to 90° and 270° (the robot body is parallel to the OY axis of the tag), the conversion ratio along OX axis is less than the value along OY axis (the tag image becomes a rectangle that has edge along OY axis longer than the edge along OX axis while in reality, the two edges are equal).

Table 2. Pose errors in the cases with different distances between tag center and image center

Cases	Δd (m)		$\Delta\theta$ (deg)	
1	P1: 0.077	P5: 0.066	P1: 1.1	P5: 1.2
2	P2: 0.158	P6: 0.037	P2: 1.5	P6: 1.7
3	P3: 0.071	P7: 0.058	P3: 1.2	P7: 1.3
4	P4: 0.147	P8: 0.046	P4: 1.2	P8: 1.1

The robot localization using AprilTags gives us stable pose reading with the position errors is less than 20 cm and heading angle error is less than 5° with our setup of tag size and vertical distance between the camera and the AprilTags.

6. Conclusion

By integrating the AprilTags into the localization function of the Vibot-2 AMR, we have greatly reduced the risk of losing the robot position during its navigation process as well as improved the accuracy and stability for the robot pose estimation.

The use of AprilTags on the one hand provides a stable and safe localization solution. Even under poor lightning conditions, the tag reading from the camera can still

give stable outputs with low errors. On the other hand this method also has some drawbacks. The accuracy of the AprilTag reading depends greatly on the quality of the camera and the motions of the robot. In most of the time, sucessfully readings only occurs with slow moving speed of the robot, otherwise fast robot motions will generate jittering in the input image stream which makes the robot fail to get infomation from the AprilTags or sometimes produce large errors which is also dangerous. Due to the limitation of the camera field of view, if the robot arrives at a position which is quite far from the destinated coordinates where a tag was mounted on the ceiling, a successfully reading will not be guaranteed. This is why we have proposed a solution to place the AprilTags along the robot path to inrease the probablity of valid reading and prevent the robot falling into a kidnapping state. As long as we can keep track of the pose validation and do the pose correction using AprilTags in time, the AMR will be able to work properly.

In our future works, we will try to improve the stability and accuracy of the robot localization algorithm by replacing the camera with better quality and integrating more advanced image processing techniques to reduce the noise created from the robot motions as well as adding location aiding devices such as radio-based GPS indoors.

Acknowledgment

The reasearch leading to these results has received funding from the Vietnam National Project No. ĐTĐLCN.45/20.

References

[1] Roland SS, Illah RN, and Davide S, "Introduction to Autonomous Mobile Robots," MIT press, second edition, 2011.

[2] Thrun S, Burgard W, and Fox D, "Probabilistic robotics," MIT press, 2005.

[3] Thrun S, Fox D, Burgard W, and Dellaert F, "Robust Monte Carlo localization for mobile robots," *Artificial intelligence*, Vol. 128, No. 1-2, pp. 99-141, 2001. https://doi.org/10.1016/S0004-3702(01)00069-8

[4] Li T, Sun S, Sattar TP, "Adapting sample size in particle filters through KLD-resampling", *Electronics Letters*, 49(12), pp. 740-742, 2013. https://doi.org/10.1049/el.2013.0233

[5] Kucner TP, Magnusson M, and Lilienthal AJ, "Where am I? An NDT-based prior for MCL", *Proceedings of the European Conference on Mobile Robots (ECMR)*, Sept. 2015. http://dx.doi.org/10.1109/ECMR.2015.7324175

[6] Richard H, Sebastian B, Sebastian O and Andreas Z, "Vector-AMCL - Vector Based Adaptive Monte Carlo Localization for Indoor Maps", *Intelligent Autonomous Systems 14, IAS 2016, Advances in Intelligent Systems and Computing*, Vol. 531, Springer Cham. http://dx.doi.org/10.1007/978-3-319-48036-7_29

[7] Sun L, Adolfsson D, Magnusson M, Andreasson H, Posner I and Duckett T, "Localising Faster: Efficient and precise lidar-based robot localisation in large-scale environments", *ArXiv*, Vol. abs/2003.01875, 2020. https://doi.org/10.48550/arXiv.2003.01875

[8] Xu S and Chou W, "An Improved Indoor Localization Method for Mobile Robot Based on WiFi Fingerprint and AMCL", *International Symposium on Computational Intelligence and Design (ISCID)*, Vol. 1, pp. 324-329, 2017. https://doi.org/10.1109/ISCID.2017.25

[9] Xu L, Baoding Z, Panpan H, Weixing X, Qingquan L, Jiasong Z and Li Q, "Kalman Filter-Based Data Fusion of Wi-Fi RTT and PDR for Indoor Localization", *IEEE Sensors Journal*, Vol. 21, No. 6, 2021. https://doi.org/10.1109/JSEN.2021.3050456

[10] Su Z, Zhou X, Cheng T, Zhang H, Xu B, and Chen W, "Global localization of a mobile robot using lidar and visual features", *IEEE International Conference on Robotics and Biomimetics (ROBIO)*, pp. 2377-2383, 2017. https://doi.org/10.1109/ROBIO.2017.8324775

[11] Nayabrasul S, Matthias L, Christian S, "2D Localization in large areas using inexpensive RGBD camera augmented with visual tags", *IEEE International Conference on Emerging Technologies and Factory Automation (ETFA 2020)*. https://doi.org/10.1109/ETFA46521.2020.9211882

[12] Michail K, Sabrina C, Anand A, Camden W, Nikolaos V, "Experimental comparison of fiducial markers for pose estimation", *International Conference on Unmanned Aircraft Systems (ICUAS 2020)*. https://doi.org/10.1109/ICUAS48674.2020.9213977

[13] Bernd P and Kostas D, "TagSLAM: Robust SLAM with Fiducial Markers", *CoRR Journal*, 2019. https://doi.org/10.48550/arXiv.1910.00679

[14] Edwin O, "AprilTag: A robust and flexible visual fiducial system", *IEEE International Conference on Robotics and Automation (ICRA 2011)*. https://doi.org/10.1109/ICRA.2011.5979561

[15] John W and Edwin O, "AprilTag 2: Efficient and robust fiducial detection", *IEEE International Conference on Intelligent Robots and Systems (IROS 2016)*. https://doi.org/10.1109/IROS.2016.7759617

[16] Jan K, Bianca F and Hans-Joachim W, "Determining and Improving the Localization Accuracy of AprilTag Detection", *IEEE International Conference on Robotics and Automation (ICRA 2020)*. https://doi.org/10.1109/ICRA40945.2020.9197427

[17] Navid K, Adam H, Wenda Z, Mohammad N, Brenda M and Angela P. S, "Improved Tag-based Indoor Localization of UAVs Using Extended Kalman Filter", *36th International Symposium on Automation and Robotics in Construction (ISARC 2019)*. http://dx.doi.org/10.22260/ISARC2019/0083

[18] Alexandre de Oliveira J, Luis P, Eduardo Giometti B and Paulo L, "Improving the Mobile Robots Indoor Localization System by Combining SLAM with Fiducial Markers", *2021 Latin American Robotics Symposium (LARS), 2021 Brazilian Symposium on Robotics (SBR), and 2021 Workshop on Robotics in Education (WRE)*. https://doi.org/10.1109/LARS/SBR/WRE54079.2021.9605456

[19] Lei Y, Mengning L and Guangyao P, "Indoor Localization Based on Fusion of AprilTag and Adaptive Monte Carlo", *2021 IEEE 5th Information Technology, Networking, Electronic and Automation Control Conference (ITNEC 2021* https://doi.org/10.1109/ITNEC52019.2021.9587205

MỘT PHƯƠNG PHÁP ĐỊNH VỊ CHO RÔ BỐT DI ĐỘNG SỬ DỤNG THẺ ĐỊNH VỊ APRILTAGS

Hoàng Văn Tiến, Tăng Quốc Nam, Trương Xuân Tùng, Nguyễn Đình Quân

Tóm tắt: *Định vị là một trong những chức năng quan trọng nhất đối với các hệ thống rô bốt tự hành (AMRs). Ở các ứng dụng hoạt động trong nhà, bài toán định vị gặp phải một số khó khăn như sự thay đổi của điều kiện ánh sáng, các đối tượng di động hoặc những bề mặt có độ phản xạ cao tạo ra các nhiễu đo đối với hệ thống nhận biết môi trường xung quanh của rô bốt. Giải pháp ước lượng tư thế của rô bốt tự hành sử dụng các thẻ định vị đang dần trở thành phổ biến và được ứng dụng hiệu quả. Trong bài báo này, chúng tôi cũng sử dụng thẻ định vị AprilTag dán trên trần cho các ứng dụng sử dụng AMR. Ưu điểm của các thẻ AprilTag đó là chúng ít bị ảnh hưởng bởi điều kiện ánh sáng, cung cấp những phép đo ổn định với dải khoảng cách đọc khá rộng từ camera quan sát đến vị trí đặt thẻ. Bằng cách tích hợp các thẻ định vị AprilTag vào gói công cụ SLAM, chúng tôi đã giải quyết được một số bài toán như vấn đề tìm lại vị trí của rô bốt trong bản đồ toàn cục và nâng cao độ chính xác của bộ tính toán định vị. Các thực nghiệm với một hệ thống rô bốt tự hành Vibot-2 AMR trong hai trường hợp: dưới điều kiện ánh sáng ban ngày và ban đêm, được tiến hành để đánh giá lại độ chính xác của phương pháp. Bên cạnh đó, chúng tôi cũng bàn đến giải pháp bố trí các thẻ định vị để tăng sự ổn định trong bài toán định vị dẫn đường của hệ thống rô bốt. Kết quả thực nghiệm cho thấy độ chính xác trong ước lượng tư thế của rô bốt nhỏ hơn 20 cm về vị trí và nhỏ hơn 5° về định hướng. Bên cạnh đó, phép đo từ camera cho kết quả khá ổn định dưới điều kiện ánh sáng thay đổi.*

Từ khóa: Rô bốt tự hành; định vị; dẫn đường; AprilTags.

Received: 19/04/2022; *Revised:* 10/10/2022; *Accepted for publication:* 11/11/2022

❑